Dermatology Practical & Conceptual

Correlation of Vascular Patterns in Skin Lesions with LC-OCT and Dermoscopy with a Tridimensional Perspective: A Pilot Study

Clément Lenoir[1], Mariano Suppa[2,3], Susana Puig[1], Véronique del Marmol[2], Raquel Albero[4], Llucia Also[4], Carmen Orte Cano[2], Gwendoline Diet[2], Margot Fontaine[2], Linda Tognetti[5], Elisa Cinotti[3,5], Pietro Rubegni[5], Jean Luc Perrot[6], Josep Malvehy[1], Javiera Perez-Anker[1]

1 Dermatology Department, Hospital Clínic de Barcelona, Universitat de Barcelona, IDIBAPS, Barcelona, Spain
2 Department of Dermatology, Hôpitaux Universitaires de Bruxelles, Université Libre de Bruxelles, Brussels, Belgium
3 Groupe d'Imagerie Cutanée Non Invasive (GICNI) of the Société Française de Dermatologie (SFD), Paris, France
4 Pathology Department, Hospital Clínic de Barcelona, Universitat de Barcelona, Barcelona, Spain
5 Dermatology Unit, Department of Medical, Surgical and Neurological Sciences, University of Siena, Siena, Italy
6 Department of Dermatology, University Hospital of Saint-Etienne, Saint-Etienne, France

Key words: LC-OCT, Dermoscopy, Vascular Pattern, Skin Lesion, Skin Imaging

Citation: Lenoir C, Suppa M, Puig S, et al. Correlation of Vascular Patterns in Skin Lesions With LC-OCT and Dermoscopy With a Tridimensional Perspective: A Pilot Study. *Dermatol Pract Concept*. 2025;15(3):5297. DOI: https://doi.org/10.5826/dpc.1503a5297

Accepted: April 8, 2025; **Published:** July 2025

Funding: None.

Competing Interests: None.

Authorship: All authors have contributed significantly to this publication.

Corresponding Author: Clément Lenoir, MD, Department of Dermatology, Hospital Clínic de Barcelona, C. de Villarroel 170, 08036 Barcelona, Spain. E-mail: clement.lenoir@outlook.com

ABSTRACT

Introduction: Vascular patterns play a crucial role in the diagnosis and differentiation of skin lesions by providing insight into underlying pathology and aid in distinguishing between benign and malignant lesions. While dermoscopy has proven valuable for visualizing these vascular structures, line-field confocal optical coherence tomography (LC-OCT) offers high-resolution, 3-dimensional (3D) imaging of the skin, potentially providing detailed visualization of vascular architecture and new insights into their projection in dermoscopy.

Objectives: This pilot study aimed to investigate the correlation between vascular patterns in skin lesions with LC-OCT and dermoscopy and explored tridimensional imaging in assessing microvascular architecture.

Methods: A cohort of patients with 14 diverse skin lesions showing typical dermoscopic vascular patterns were examined using dermoscopy and LC-OCT. LC-OCT images were analyzed, and manual segmentation with tridimensional reconstruction of the vascular structures was performed. The correlation between these vascular structures and their dermoscopic projection was then assessed qualitatively.

Results: LC-OCT demonstrated a strong visual correlation with dermoscopy in identifying vascular patterns, offering additional depth and 3D details of the intricate relationship between skin micro-architecture and the development of specific vascular patterns in skin lesions.

Conclusions: LC-OCT correlates with dermoscopy in vascular pattern analysis in skin lesions. The added advantage of 3D imaging helped us understand the way vascular structures are formed in skin lesions depending on their micro-architecture. LC-OCT could potentially play a significant role in precisely assessing the vascular environment of skin lesions. Further studies are necessary to assess how this could provide clinical value for diagnosing or monitoring skin lesions.

Introduction

The accurate diagnosis and assessment of skin lesions are crucial for effective patient management, and naked-eye examination is, in many cases, insufficient to differentiate between benign and malignant skin conditions, not to mention to achieve a correct diagnostic. The advent of dermoscopy in the early 1980s has revolutionized daily dermatological practice by providing a time- and cost-efficient tool that has significantly enhanced early detection of skin cancer, leading to improved patient outcomes [1-6]. Moreover, dermoscopy assists in reducing unnecessary excisions, selecting the appropriate biopsy site, and monitoring suspicious lesions over time and is also increasingly being used in the field of inflammatory dermatoses, onychology, and trichology [7-11].

With the identification of specific features such as pigment network, globules, streaks, and various vascular patterns, the dermoscopist can in many cases confidently differentiate benign lesions from potentially malignant ones [1,6,12-14]. The study of vascular patterns encompasses a wide chapter in the field of dermoscopy as these patterns are indicative of certain diagnoses, with varying sensitivity and specificity [15-16]. In particular, vascular patterns are of paramount diagnostic relevance in hypopigmented lesions, where pigment-based criteria may be less discernible [15-17].

As more sophisticated skin-imaging techniques have been made available in the recent years, the visualization of the skin at a microscopical scale and in vivo allows a much more insightful understanding of the skin architecture, including of its microcirculation. Reflectance confocal microscopy (RCM) was the first technology to provide in vivo cellular resolution of skin lesion vascularization, though limited by the shallow penetration depth and a solely horizontal display [18-19]. The newly developed line-field confocal optical coherence tomography (LC-OCT) displays a tridimensional image of the skin combining the high isotropic resolution of RCM and the penetration depth of standard OCT [20]. With these technical assets, LC-OCT stands out as a potentially ideal tool to study in vivo the vascular microstructure of the skin and its alterations in pathological conditions [21-23].

Objectives

This pilot study aimed to qualitatively correlate the different vascular patterns observed in dermoscopy examination of a range of common skin lesions with real-time in vivo LC-OCT acquisitions. We hypothesized that LC-OCT could reveal tridimensional microvascular architectures corresponding to known dermoscopic vascular patterns, thereby improving our understanding of how these patterns project in 2D view.

Methods

From June 2023 to March 2024, we prospectively evaluated adult patients who consulted for evaluation of various skin lesions in the regular workflow of the department. Patients presenting with skin lesions that exhibited vascular patterns classically described in dermoscopy literature were prospectively selected for inclusion. The selection aimed to assemble a representative and didactic panel of common vascular morphologies based on established criteria from key dermoscopic reviews [15-16]. The patients consented to undergo examination with LC-OCT, either as recommended by the dermatologist for diagnostic purposes or for the sole interest of this study. The fourteen selected cases include a cherry angioma displaying red lacunas, a sebaceous glandular hyperplasia showing crown vessels, a nodular basal cell carcinoma (BCC) displaying arborizing vessels, a superficial BCC and an infiltrative one showing short fine telangiectasias, a seborrheic keratosis (SK) with hairpin vessels, a clear cell acanthoma (CCA) with the typical string of pearls vascular pattern, a Bowen disease lesion with glomerular vessels, a dermal nevus with comma vessels, an atypical nevus with dotted vessels, an invasive melanoma showing milky-red areas, a second invasive melanoma displaying linear irregular

vessels, and finally, both an invasive melanoma and a squamous cell carcinoma (SCC) with polymorphous vessels.

Acquisitions were collected using the LC-OCT device (deepLiveTM, DAMAE Medical, Paris, France). The lesions were mapped using the high resolution with broad field of view dermoscope and then explored in vertical view using the integrated videodermoscopy camera. Several tridimensional blocks (1.2 × 0.5 × 0.4 mm) were acquired from the regions of interest presenting the most typical vascular patterns.

The 3D stack images acquired from LC-OCT were converted into a "negative" image to make the vessels appear brighter against the surrounding tissue. When the resulting picture allowed clear delineation of the vessel compared to the surrounding tissue, the SNT (Simple Neurite Tracer) plugin of the ImageJ software was used to manually draw the skeleton of each vessel. This process was performed in 2D projections of the stack from three different orientations: sagittal, frontal, and horizontal. Each vessel was traced meticulously to ensure accuracy. All segmentations were performed manually by a single experienced operator to ensure consistency across cases. Once all vessels were drawn, a binary mask of the traced vessels was exported. This binary mask was then smoothed to generate a 3D representation of the vascular architecture. This 3D model allowed for detailed analysis and visualization of the microvascular patterns within the skin lesions. This manual segmentation was provided in all but the two cases that were not suitable for this process, which requires a clear contrast in reflectivity between the vessels and the surrounding stroma.

All the examined lesions underwent biopsy or excision for diagnostic confirmation, therapeutic and/or aesthetic purposes requested by the patient. This comprehensive methodology allowed us to correlate dermoscopic vascular patterns with the 3D microarchitectural counterparts using LC-OCT of histologically diagnosed lesions.

Results

Red Lacunae

Red lacunae are a characteristic feature commonly observed in benign angiomas [24]. Dermoscopically, these structures appear as well-defined, homogeneous red areas reflecting the presence of dilated blood-filled spaces within the lesion [25]. In LC-OCT imaging, red lacunae correspond to large, well-circumscribed hyporeflective vascular spaces located in the dermis. The regular distribution and size of these structures underscore the benign nature of the lesion (Figure 1).

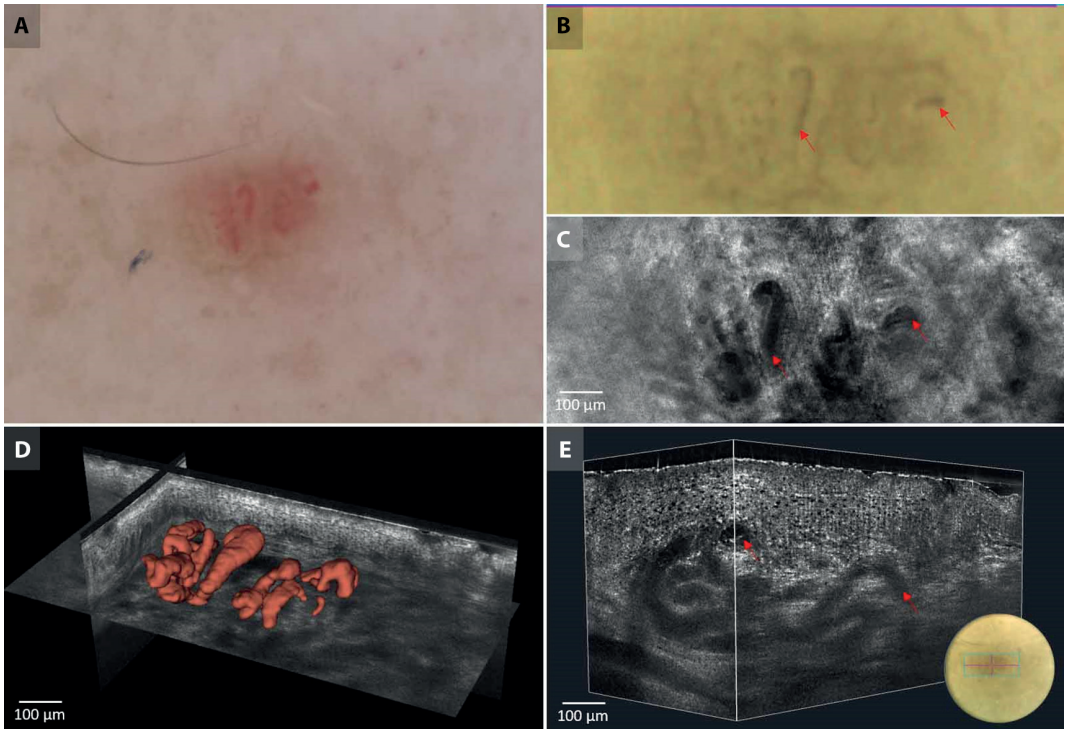

Figure 1. Red lacunae in cherry angioma. (A) Dermoscopic, (B) LC-OCT-integrated dermoscopic colocalization, (C) LC-OCT horizontal view, (D) tridimensional segmentation reconstruction, and (E) LC-OCT tridimensional block presentations. LC-OCT examination reveals large, well-circumscribed hyporeflective vascular spaces.

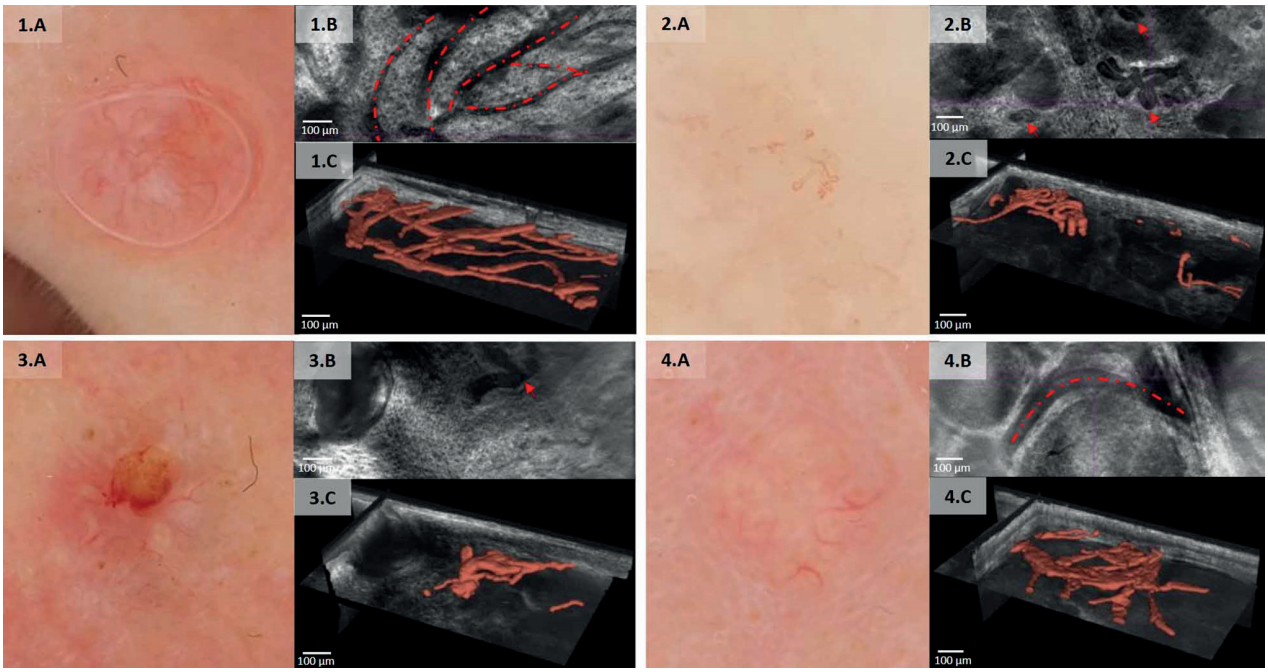

Figure 2. Arborizing vessels in nodular basal cell carcinoma (BCC) (1), short fine vessels in superficial BCC (2), combination of both in infiltrative BCC (3) and crown vessels in sebaceous glandular hyperplasia (4). For each lesion, the (A) dermoscopic picture, (B) LC-OCT horizontal view, and (C) tridimensional segmentation reconstruction are presented. Nodular BCC (1): LC-OCT examination reveals tree-like branching of arborizing vessels, weaving around and over the tumor lobules. Superficial BCC (2): LC-OCT examination reveals short and fine capillary vessels intertwined within the stroma and around the tumor nests. Infiltrative BCC (3): LC-OCT examination shows short, fine vessels associated with larger arborizing-like vessels within the stroma and weaving around infiltrative tumor nests. Sebaceous hyperplasia (4): LC-OCT examination shows linear, crown-like vessels arranged radially and around the glandular structures.

Crown Vessels

Crown vessels are a distinct vascular pattern predominantly found in sebaceous glandular hyperplasia [15]. These vessels are characterized by linear, curved configurations with minimal branching positioned along the periphery of the lesion and extending toward the center without crossing it, thereby creating a crown-like appearance [25]. LC-OCT reveals these dilated vessels in the superficial dermis, of regular caliber, and uniformly contouring the regularly distributed dilated glandular structures. The vessels maintain a horizontal orientation, projecting as crown shapes in dermoscopy (Figure 2).

Arborizing Blood Vessels

Arborizing vessels represent a key vascular pattern most notably observed in nodular BCC through dermoscopy [15,26]. These vessels exhibit a distinctive morphology characterized by irregular, tree-like branching [25]. In-depth examination of this nodular BCC using LC-OCT reveals prominently dilated and tortuously branched vessels, intricately weaving around and crossing over the tumor lobules within the dermis. The spatial constraints of the overlying epidermis and the underlying tumor lobules result in a compression of these capillaries, hence appearing flattened just underneath the basal membrane in the LC-OCT imaging, explaining their appearance as sharply focused vessels crossing over the tumor lobules in dermoscopy (Figure 2).

Short Fine Telangiectasias

The short fine telangiectasia vascular pattern is a feature frequently identified through dermoscopy in all subtypes of BCC, though more indicative of superficial and infiltrative subtypes than of nodular [15,26-28]. These vessels appear shorter and finer compared to the more prominent arborizing vessels typically seen in nodular BCC [25]. LC-OCT of both these cases of superficial and infiltrative (Figure 2) BCCs reveals fine capillaries dispersed and intertwined around the tumor nests and within the surrounding stroma. In the infiltrative subtype these vessels were associated with a larger arborizing-like vessel.

Hairpin Vessels

The hairpin vessel vascular pattern is a common, characteristic finding in dermoscopy, frequently observed in keratinizing tumors, SK being the most frequent one [15,24,29]. These hairpin vessels appear as loop-like projections, sometimes surrounded by a whitish halo [25].

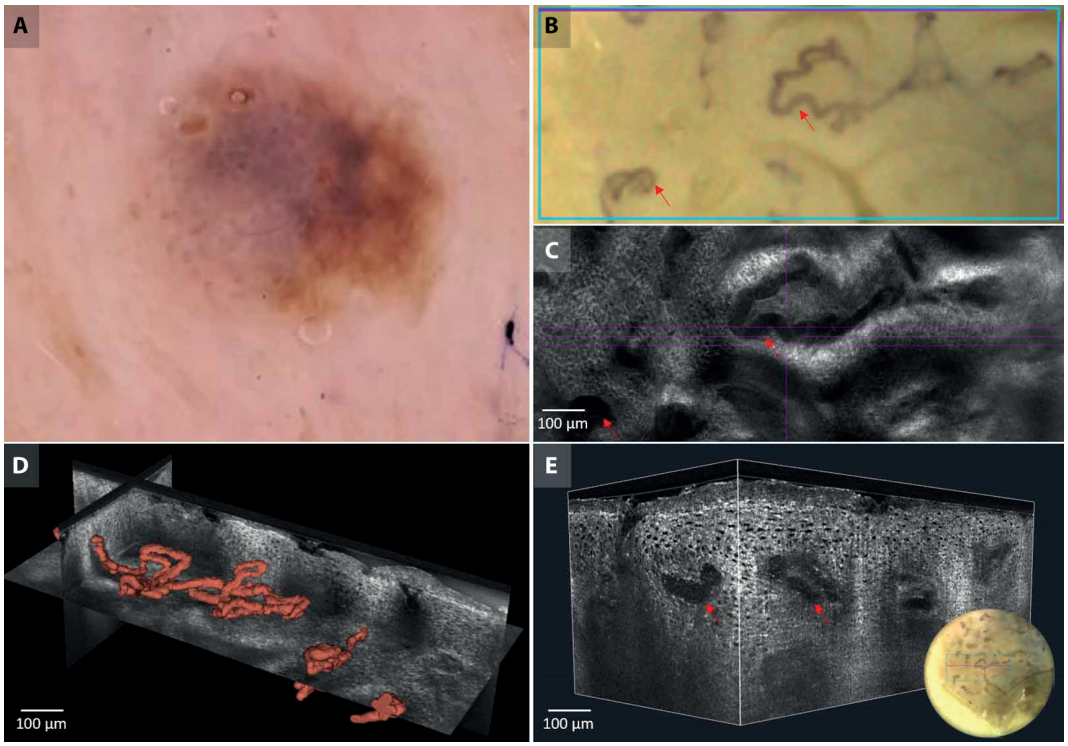

Figure 3. Hairpin vessels in seborrheic keratosis. (A) Dermoscopic, (B) LC-OCT-integrated dermoscopic colocalization, (C) LC-OCT horizontal view, (D) tridimensional segmentation reconstruction, and (E) LC-OCT tridimensional block presentations. LC-OCT examination shows the capillary vessels orientated as and loop projections vertically and diagonally within the dermal papillae.

High-resolution imaging with LC-OCT reveals dilated capillary vessels emerging within elongated dermal papillae and displaying various vertical orientations depending on the surrounding tumoral architecture that shapes the underlying dermis. The shape of the loop horizontally projects as the hairpin-like structure observed in dermoscopy (Figure 3).

String of Pearls Pattern

The "string of pearls" vascular pattern is a specific feature characterized by dotted or glomerular vessels arranged in a serpiginous distribution, resembling a string of pearls. This pattern is highly indicative of CCA [15,25,32,40]. LC-OCT acquisitions of this case reveal mildly glomerular vessels regularly arranged within the dermal papillae, themselves distributed in a linear serpentine manner and surrounded by homogenous acanthosis without pleiomorphism, mirroring the serpiginous aspect of these vessels observed in dermoscopy (Figure 4).

Glomerular Vessels

Glomerular vessels are a characteristic dermoscopic vascular pattern most observed in Bowen's disease1 and presenting as roundish, glomerulus-like structures [5,24,33]. LC-OCT offers a detailed visualization of these vessels, revealing their typical coiled shape within the dermal papillae, wholly surrounded by the acanthotic and pleiomorphic keratinocytic proliferation. In both vertical and horizontal LC-OCT sections, as well as in 3-dimensional reconstructions, the glomerular vessels maintain their distinctive morphology, corresponding to the projections described in dermoscopy (Figure 5).

Comma Vessels

Comma vessels are a distinctive vascular pattern predominantly observed in dermal nevi, usually curved and not as sharply focused as seen in BCC [16,25,35,36]. LC-OCT provides a detailed view of these vessels, revealing their horizontalized, curved morphology within the superficial dermis. These vessels are situated around nests of nevocytes, with a regular and roundish caliber. The horizontal orientation of comma vessels reflects the predominant localization of melanocytic proliferation within the dermis, with minimal junctional activity. This anatomical positioning allows the vessels to maintain a regular horizontal shape beneath the epidermis (Figure 6).

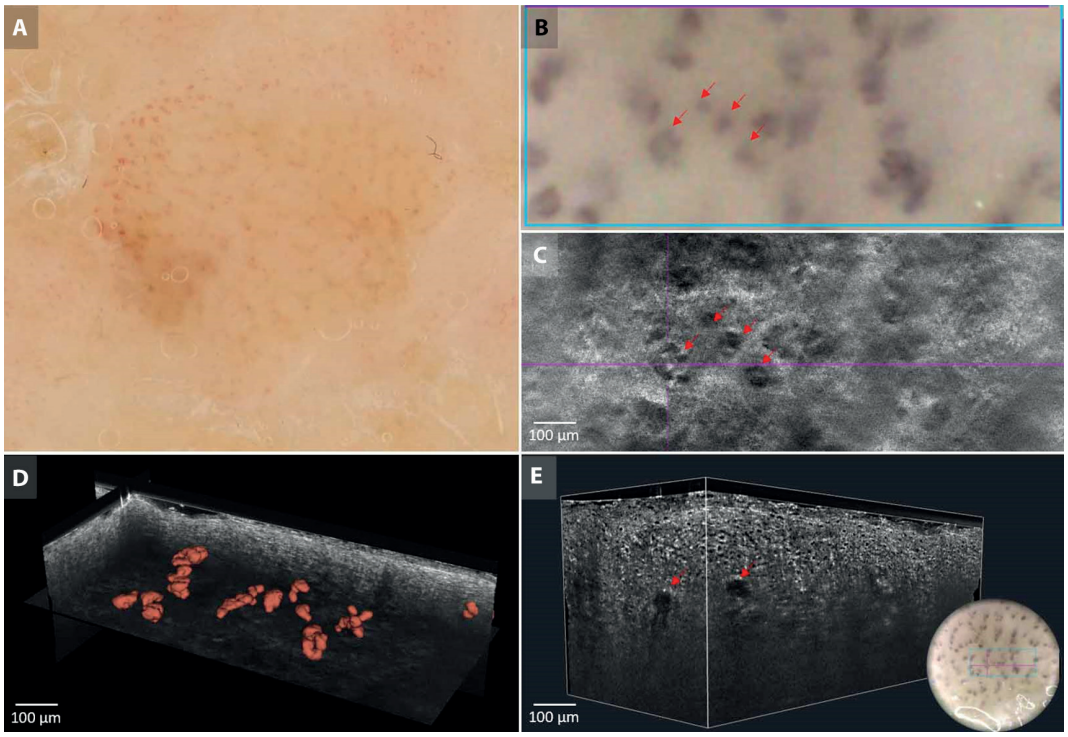

Figure 4. String of pearls pattern in clear cell acanthoma. (A) Dermoscopic, (B) LC-OCT-integrated dermoscopic colocalization, (C) LC-OCT horizontal view, (D) tridimensional segmentation reconstruction, and (E) LC-OCT tridimensional block presentations. LC-OCT examination reveals small glomerular vessels distributed in a serpiginous pattern following the disposition of dermal papillae within the regularly acanthotic epidermis.

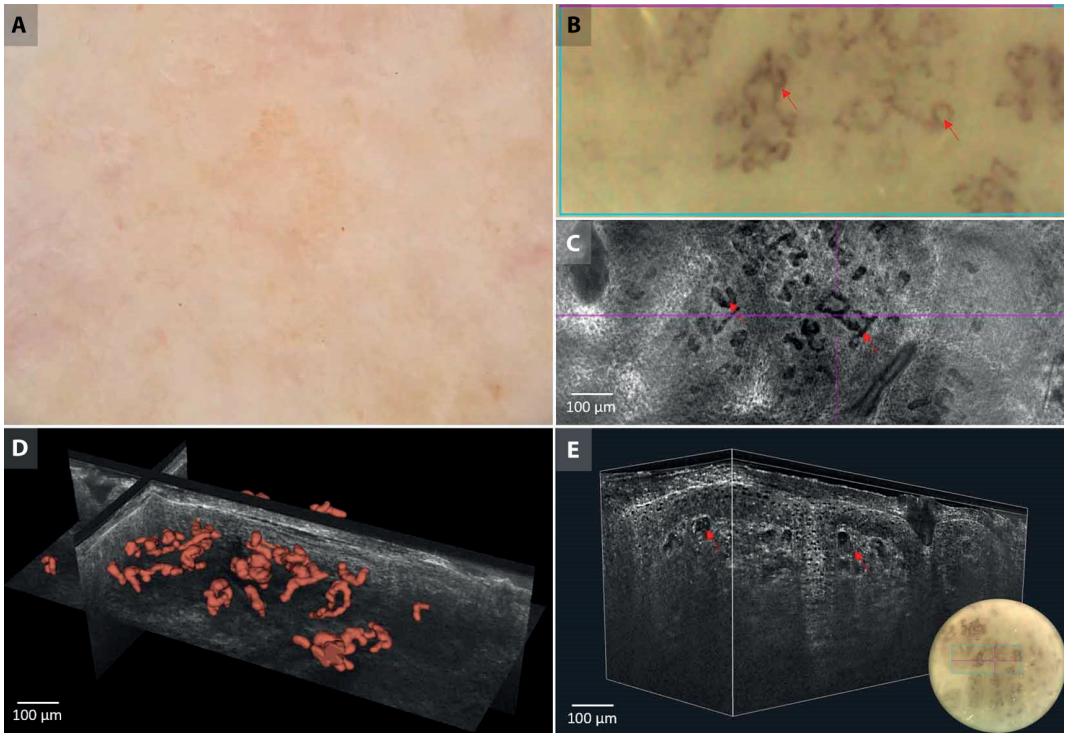

Figure 5. Glomerular vessels in Bowen disease. (A) Dermoscopic, (B) LC-OCT-integrated dermoscopic colocalization, (C) LC-OCT horizontal view, (D) tridimensional segmentation reconstruction, and (E) LC-OCT tridimensional block presentations. LC-OCT examination displays coiled, glomerular vessels within the dermal papillae, distributed within the acanthotic and dysplastic keratinocytic proliferation.

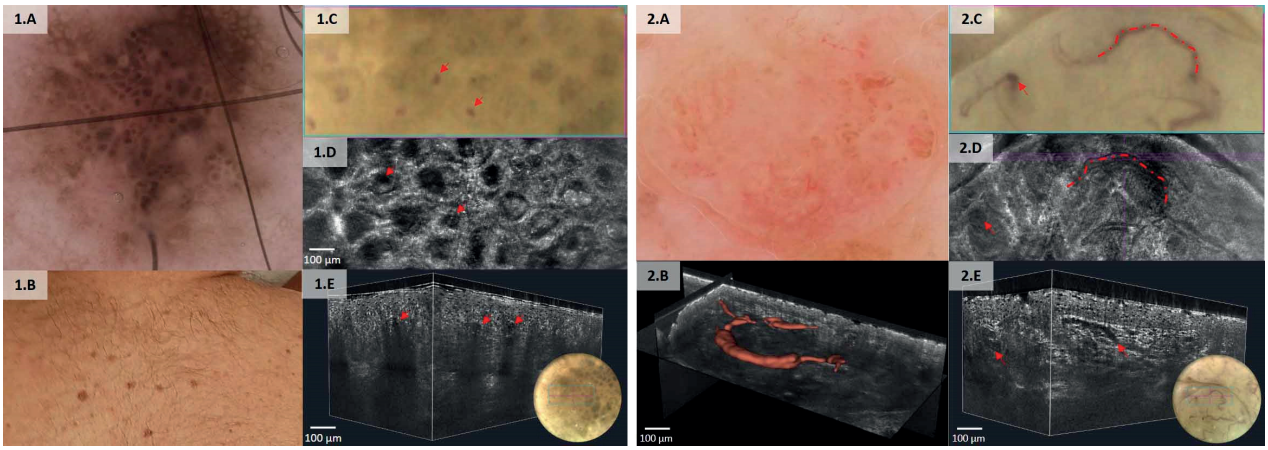

Figure 6. Dotted vessels in atypical nevus (1) and comma vessels in dermal nevus (2). For each lesion, the (A) dermoscopic picture, (B) LC-OCT-integrated dermoscopic colocalization, (C) LC-OCT horizontal view, (D) tridimensional segmentation reconstruction, and (E) LC-OCT tridimensional block are presented. Atypical nevus (1): LC-OCT examination reveals vertically oriented vessels in dermal papillae compressed within epidermal crests filled with large melanocytic nests. Segmentation was not possible for this lesion. Dermal nevus (2): LC-OCT examination reveals horizontally curved vessels around and over melanocytic nests within the dermis and under a flattened dermoepidermal junction.

Dotted Vessels

The dotted vascular pattern is commonly observed in various lesions, notably in compound or atypical melanocytic tumors [16,25,35]. In LC-OCT, the dotted vessels appear vertically oriented, compressed between the epidermal crests with junctional nests, forcing them into a vertical alignment. This contrasts with the more horizontal orientation seen in dermal nevi due to their lack of junctional activity and flattened dermoepidermal junction. The upper loops of these dotted vessels extend into the superficial dermis, projecting as the sharply focused dots observed in dermoscopy (Figure 6).

Linear Irregular Vessels

Linear irregular vessels are a distinctive vascular pattern frequently observed in melanoma [16,35]. They appear as irregular, elongated lines that abruptly change in direction and thickness, projecting more or less in focus depending on their depth, reflecting their irregular orientation [25]. The LC-OCT tridimensional reconstruction of our case shows that their shape and distribution closely revolve around the invasive melanocytic tumoral nests that proliferate in the dermis. We can observe the vessels abruptly changing orientation from a vertical direction to a horizontal one when contouring the large tumoral nests, correlating with their description in dermoscopy (Figure 7).

Milky Red Areas

Milky red areas are a notable dermoscopic feature of invasive melanomas, indicative of the intense vascular density and activity characteristic of advanced tumors [19,35,37]. Dermoscopically, these regions manifest as blurry, reddish-pale areas of varying shape and distribution [25]. The high-resolution imaging provided by LC-OCT reveals the complex microvascular environment in the superficial dermis contributing to this appearance. The precise vascular microarchitecture appears challenging to delineate due to the minimal reflectivity contrast between the small-sized vessels and the densely populated dermis invaded by tumoral and inflammatory cells. These vessels form numerous capillaries intricately intertwined within the infiltration of invasive melanoma cells (Figure 8).

Polymorphous Vessels

Polymorphous vessels are a key vascular pattern, particularly noted in invasive tumors such as melanoma and SCC [15,16,24,35,38]. These vessels display anarchically oriented, dilated structures of varying sizes and shapes, sometimes resembling other patterns such as glomerular, hairpin, or dotted vessels, and of irregular shapes and distribution [25]. LC-OCT illustrates this disarray in both our cases of melanoma and SCC (Figure 9). The former shows a network of dilated vessels intertwined with dense clusters of melanoma cells and nests within the dermis, while the latter displays enlarged and disorganized vessel clusters vaguely reminiscent of glomerular structures inside dermal papillary spaces squeezed within the invasive squamous cell proliferation.

Discussion

The preliminary results of this study provide a significant step forward in understanding the microvascular

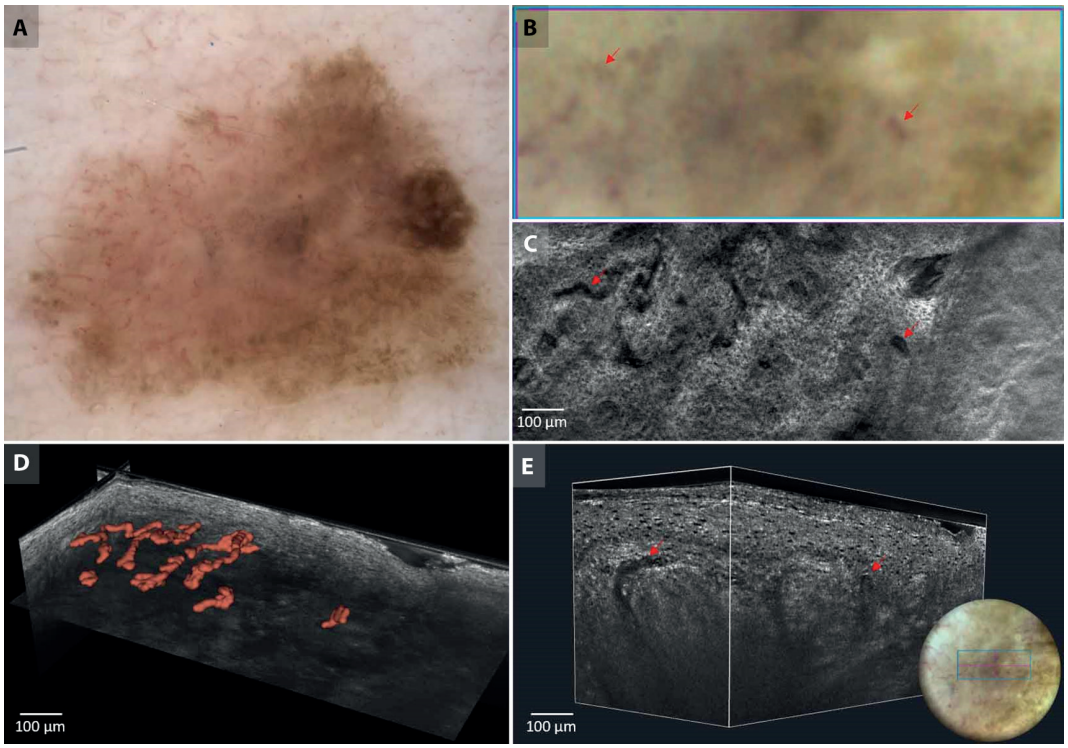

Figure 7. Linear irregular vessels in melanoma. (A) Dermoscopic, (B) LC-OCT-integrated dermoscopic colocalization, (C) LC-OCT horizontal view, (D) tridimensional segmentation reconstruction, and (E) LC-OCT tridimensional block presentations. LC-OCT examination reveals irregularly oriented vessels around large dermal and atypical melanocytic nests, sharply changing their orientation around those.

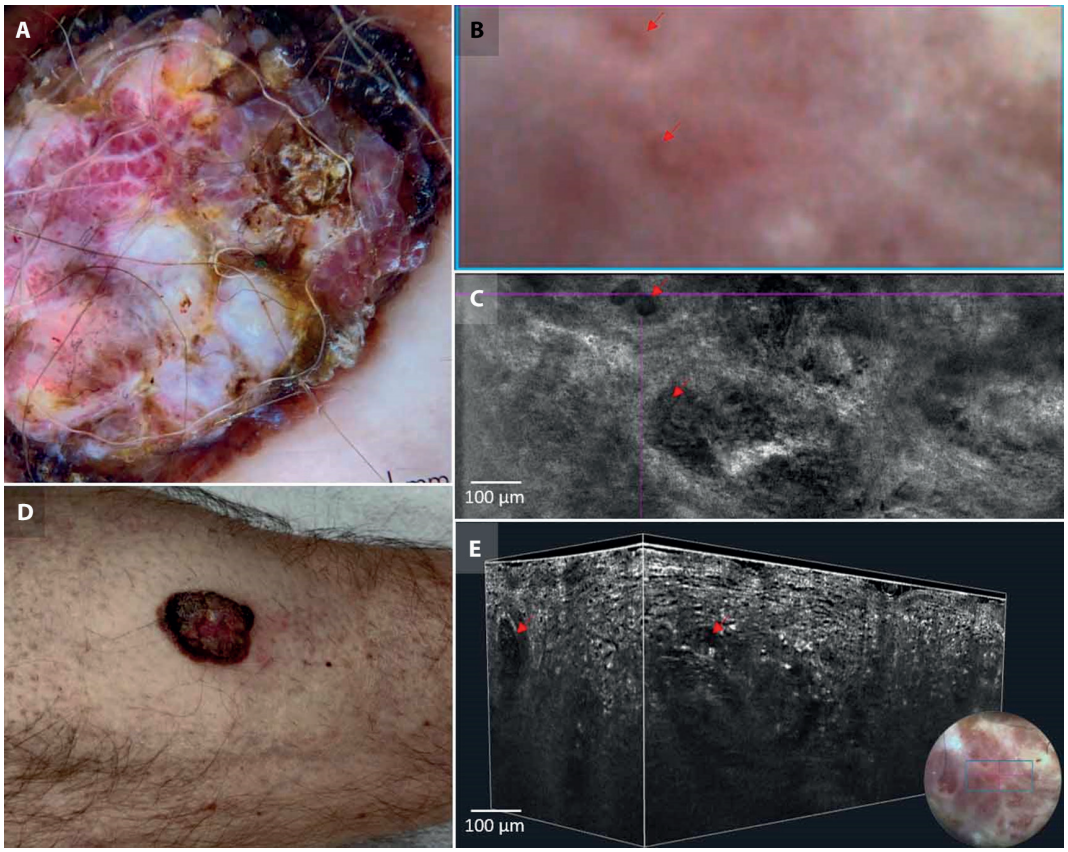

Figure 8. Milky red areas in invasive melanoma. (A) Dermoscopic, (B) LC-OCT-integrated dermoscopic colocalization, (C) LC-OCT horizontal view, (D) clinical, and (E) LC-OCT tridimensional block presentations. LC-OCT examination reveals a dense capillary network within the dermis, which is infiltrated by large pleiomorphic melanocytes and inflammatory cells. Segmentation was not possible for this lesion.

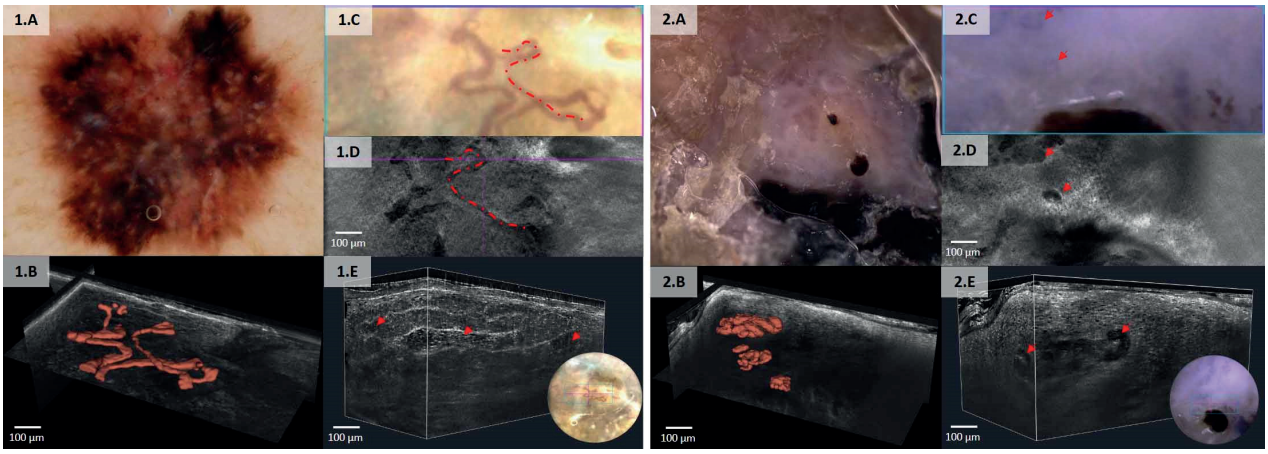

Figure 9. Polymorphous vessels in melanoma (1) and squamous cell carcinoma (2). For each lesion, the (A) dermoscopic picture, (B) LC-OCT-integrated dermoscopic colocalization, (C) LC-OCT horizontal view, (D) tridimensional segmentation reconstruction, and (E) LC-OCT tridimensional block are presented. Melanoma (1): LC-OCT examination shows dilated polymorphous and chaotic vascular structures around large invasive melanocytic tumor nests. Squamous cell carcinoma (2): LC-OCT examination reveals disorganized polymorphous vessels, some of them vaguely resembling glomerular capillaries with varying sizes and shapes, within dermal papillae in the neoplastic squamous cell proliferation.

architecture of various skin lesions and can be leveraged to conduct relevant transversal and comparative studies between and within categories of lesions. Indeed, the varying vascularization patterns could reflect significant differences in biological behavior and prognosis among types and subtypes of lesions.

It has been shown in previous histopathology-based studies that the vascularization pattern in BCC represents a relevant indicator of tumor growth profile, invasiveness, and aggressiveness [19,39-41]. BCCs display particular vascular characteristics, with blood vessels prominently situated at the tumor periphery and absent within the tumor nests, which has been hypothesized to correlate with their low metastatic potential and mainly local invasiveness [19,39,42]. The increased microvascular density (MVD) at the tumor-stroma interface is associated with more aggressive BCC subtypes, such as infiltrative and morpheaform variants [40], and a significant distinction is observed in comparison with the more indolent superficial BCC subtypes [19]. Moreover, nodular BCCs typically feature larger blood vessels with a diameter greater than 0.2 mm surrounding the tumor lobules, indicative of a higher degree of vascularization and potential for more aggressive local invasion [18-19]. In contrast, superficial BCCs have smaller and fewer blood vessels, generally with a diameter less than 0.2 mm, which seems to correlate with their lower risk and less invasive nature [18-19].

LC-OCT has provided in vivo detailed insights into the three-dimensional architecture of the vascular networks within these lesions. The arborizing vessels in nodular BCC were observed as prominently dilated and tortuously branched, weaving around and crossing over the tumor lobules within the dermis, whereas in the superficial BCC, LC-OCT displayed finer capillaries dispersed around the lobules within the surrounding stroma. The infiltrative subtype is infamously considered the hardest to diagnose in daily clinical practice [27,43]. However, the co-existence of arborizing vessels with short fine telangiectasia, as in our case, showed a certain level of specificity in previous studies [44-46]. Specific and objective criteria regarding vessel caliber, density, and distribution in BCCs are yet to be defined to carry any clear prognostic value in terms of tumor aggressiveness. However, thanks to the microscopic histology-like tridimensional acquisitions that it provides, we believe that LC-OCT has the potential to give precise measurements of these parameters, which could open the way to further studies on the topic.

Keratinizing lesions also show variability in their vascular patterns despite more similarity in their overall architecture, all of them sharing potential for acanthosis and hyperkeratosis. Bowen disease usually displays regularly distributed glomerular capillaries within the dermal papillae, which appear thinned and entrapped in an acanthotic and dysplastic epidermis [15,33,34]. Vessels in CCA appear as dotted or glomerular capillaries with a serpiginous distribution within dermal papillae surrounded by a regular acanthotic epidermis but without the keratinocytic dysplasia found in Bowen disease [15,31,32]. In SCC, vascular

architecture appears more chaotic and irregular, but some vessels retain a vaguely enlarged and irregular glomerular aspect, emphasizing the possible progression from an in situ carcinoma towards invasive carcinoma. Interestingly, seborrheic keratoses, which can exhibit similar morphology with previously described lesions and show varying levels of acanthosis and hyperkeratosis, commonly display vessels shaped as hairpin rather than glomerular [15,29]. These vessels loop within the thinned dermal papillae, squeezed vertically or diagonally by the acanthotic epidermis around. The exact biological mechanisms driving these distinct vascularization patterns within keratinizing tumors remain to be elucidated as morphology of the epidermal proliferation seems not to be the only defining factor.

Melanocytic lesions display a more diverse range of vascular characteristics based on their subtype and aggressiveness. As observed in LC-OCT, dermal nevi typically show horizontalized vessels along a junction that is free of melanocytic nests. In compound and atypical nevi, increased junctional activity often shapes the vessels vertically, compressing them inside the thinned dermal papillae and projecting them as sharply focused dots in dermoscopy. The development of invasive melanoma starkly differs from that of BCC by the much more disorganized and intense neovascular network supporting it, including increased intratumoral vascularization spreading into and within the tumor nests, as opposed to BCC [19]. Moreover, vessel density and pattern in melanomas are indicative of their aggressive behavior, with higher MVD and the presence of complex vascular structures, projecting as polymorphous vessels or milky-red areas in dermoscopy, being associated with poorer prognosis [37,47]. The increased neoangiogenesis seen in melanomas seems to facilitate their invasive potential, enabling deeper penetration into the dermis and increasing the likelihood of metastasis [37]. These vascular characteristics thus appear crucial in assessing their biological behavior and prognosis. The use of dynamic OCT has already been studied for the assessment of vascular activity in melanoma, showing that blood vessel density and atypical shapes increased with higher tumor stage [48,49]. However, it failed to provide accurate correlation with dermoscopy [48]. We believe that LC-OCT, by offering microscopic and tridimensional visualization of the complex microvascular environment in melanoma, has the potential to precisely correlate with dermoscopy and to measure parameters that could reflect the vascular activity of these lesions as well as possibly provide relevant prognostic information. Further studies will be needed to verify these hypotheses.

The primary manual delineation of these patterns is crucial to feeding an AI algorithm designed to facilitate the process. Although segmentation was performed by a single experienced operator to ensure consistency, interobserver variability was not assessed and should be addressed in future studies. Moreover, the process is especially challenging in cases where the vascular structures overall have comparable reflectivity to the surrounding stroma, typically when numerous thin and small capillaries are found in a dermis infiltrated by neoplastic and inflammatory cells, as in the case of milky-red areas in melanoma. AI's ability to learn from these manually traced images will ultimately enhance its capacity to automatically delineate complex microvascular patterns, improving accuracy and efficiency in the analysis of skin lesions. So far, this segmentation process has allowed us to isolate the microvascular architecture in twelve of our lesions, providing a didactic panel of vascular patterns commonly observed in dermoscopy and correlated with their tridimensional reconstruction Figure 10.

Recent studies have underscored the role of stroma and its interaction with tumors as a critical aspect of understanding skin lesion vascularization and neoangiogenesis. Tumor-associated stromal cells, such as fibroblasts and inflammatory cells, secrete growth factors, cytokines, and enzymes that modulate the tumor microenvironment and promote angiogenesis [50-54]. Except for a few already available oncology treatments centered around tumoral neoangiogenesis [55], the implication of this knowledge in clinical practice is not yet fully established. We believe that the ability of LC-OCT to bridge clinical and dermoscopy with cellular resolution microscopy and to elucidate the vascular microarchitecture of pathological processes with unparalleled realism could also provide crucial morphological insights into the biology driving lesion vascularization. As a pilot study with a small sample size, the findings are mostly exploratory. Further descriptive and quantitative studies with larger cohorts, reinforced by the development of AI algorithms for more precise and easy definition of microvascularization, are expected to add more pieces to the puzzle. This study was not designed to assess whether LC-OCT influences lesion management, but rather to provide a morphological framework that could support future diagnostic and clinical applications. This could eventually enhance the treatment planning for various skin lesions, ultimately leading to improved patient outcomes.

Figure 10. Tridimensional segmentation of various dermoscopic vascular patterns. This figure summarizes the previously described tridimensional segmentation reconstructions of different vascular patterns correlated with their dermoscopic projection.

References

1. Kittler H, Pehamberger H, Wolff K, Binder M. Diagnostic accuracy of dermoscopy. *Lancet Oncol*. 2002;3(3):159-65. DOI: 10.1016/s1470-2045(02)00679-4. PMID: 11902502.
2. Yelamos O, Braun RP, Liopyris K, Wolner ZJ, Kerl K, Gerami P, et al. Usefulness of dermoscopy to improve the clinical and histopathologic diagnosis of skin cancers. *J Am Acad Dermatol*. 2019;80(2):365-77. DOI: 10.1016/j.jaad.2018.07.072. PMID: 30321580.

3. Chevolet I, Hoorens I, Janssens A, Speeckaert R, Van Geel N, Van Maele G, et al. A short dermoscopy training increases diagnostic performance in both inexperienced and experienced dermatologists. *Australas J Dermatol*. 2015;56(1):52-5. DOI: 10.1111/ajd.12203. PMID: 25302740.
4. Mogensen M, Jemec GB. Diagnosis of nonmelanoma skin cancer/keratinocyte carcinoma: a review of diagnostic accuracy of nonmelanoma skin cancer diagnostic tests and technologies. *Dermatol Surg*. 2007;33(10):1158-74. DOI: 10.1111/j.1524-4725.2007.33251.x. PMID: 17903149.
5. Argenziano G, Puig S, Zalaudek I, Sera F, Corona R, Alsina M, et al. Dermoscopy improves accuracy of primary care physicians to triage lesions suggestive of skin cancer. *J Clin Oncol*. 2006;24(12):1877-82. DOI: 10.1200/JCO.2005.05.0864. PMID: 16622262.
6. Giacomel J, Zalaudek I. Dermoscopy of superficial basal cell carcinoma. *Dermatol Surg*. 2005;31(12):1710-3. DOI: 10.2310/6350.2005.31314. PMID: 16336893.
7. Szebenyi J, Legradi M, Nemeth C, Joura MI, Gyulai R, Lengyel Z. Dermoscopy of inflammatory skin diseases. *Dermatologie (Heidelb)*. 2023;74(4):232-42. DOI: 10.1007/s00105-023-05122-9. PMID: 36897374.
8. Sgouros D, Apalla Z, Ioannides D, Katoulis A, Rigopoulos D, Sotiriou E, et al. Dermoscopy of Common Inflammatory Disorders. *Dermatol Clin*. 2018;36(4):359-68. DOI: 10.1016/j.det.2018.05.003. PMID: 30201145.
9. Lallas A, Zalaudek I, Argenziano G, Longo C, Moscarella E, Di Lernia V, et al. Dermoscopy in general dermatology. *Dermatol Clin*. 2013;31(4):679-94, x. DOI: 10.1016/j.det.2013.06.008. PMID: 24075553.
10. Lacarrubba F, Micali G, Tosti A. Scalp dermoscopy or trichoscopy. *Curr Probl Dermatol*. 2015;47:21-32. DOI: 10.1159/000369402. PMID: 26370641.
11. Starace M, Alessandrini A, Piraccini BM. Dermoscopy of the Nail Unit. *Dermatol Clin*. 2021;39(2):293-304. DOI: 10.1016/j.det.2020.12.008. PMID: 33745641.
12. Gouda G, Pyne J, Dicker T. Pigmented Macules on the Head and Neck: A Systematic Review of Dermoscopy Features. *Dermatol Pract Concept*. 2022;12(4):e2022194. DOI: 10.5826/dpc.1204a194. PMID: 36534577.
13. Goncharova Y, Attia EA, Souid K, Vasilenko IV. Dermoscopic features of facial pigmented skin lesions. *ISRN Dermatol*. 2013;2013:546813. DOI: 10.1155/2013/546813. PMID: 23431466.
14. Weber P, Tschandl P, Sinz C, Kittler H. Dermoscopy of Neoplastic Skin Lesions: Recent Advances, Updates, and Revisions. *Curr Treat Options Oncol*. 2018;19(11):56. DOI: 10.1007/s11864-018-0573-6. PMID: 30238167.
15. Zalaudek I, Kreusch J, Giacomel J, Ferrara G, Catricala C, Argenziano G. How to diagnose nonpigmented skin tumors: a review of vascular structures seen with dermoscopy: part II. Nonmelanocytic skin tumors. *J Am Acad Dermatol*. 2010;63(3):377-86; quiz 87-8. DOI: 10.1016/j.jaad.2009.11.697. PMID: 20708470.
16. Zalaudek I, Kreusch J, Giacomel J, Ferrara G, Catricala C, Argenziano G. How to diagnose nonpigmented skin tumors: a review of vascular structures seen with dermoscopy: part I. Melanocytic skin tumors. *J Am Acad Dermatol*. 2010;63(3):361-74; quiz 75-6. DOI: 10.1016/j.jaad.2009.11.698. PMID: 20708469.
17. Giacomel J, Zalaudek I. Pink lesions. *Dermatol Clin*. 2013;31(4):649-78, ix. DOI: 10.1016/j.det.2013.06.005. PMID: 24075552.
18. Lupu M, Caruntu C, Popa MI, Voiculescu VM, Zurac S, Boda D. Vascular patterns in basal cell carcinoma: Dermoscopic, confocal and histopathological perspectives. *Oncol Lett*. 2019;17(5):4112-25. DOI: 10.3892/ol.2019.10070. PMID: 30944604.
19. Bungardean RM, Stoia MA, Pop B, Crisan M. Morphological aspects of basal cell carcinoma vascularization. *Rom J Morphol Embryol*. 2023;64(1):15-23. DOI: 10.47162/RJME.64.1.02. PMID: 37128787.
20. Ogien J, Tavernier C, Fischman S, Dubois A. Line-field confocal optical coherence tomography (LC-OCT): principles and practical use. *Ital J Dermatol Venerol*. 2023;158(3):171-9. DOI: 10.23736/S2784-8671.23.07613-2. PMID: 37278495.
21. Suppa M, Palmisano G, Tognetti L, Lenoir C, Cappilli S, Fontaine M, et al. Line-field confocal optical coherence tomography in melanocytic and non-melanocytic skin tumors. *Ital J Dermatol Venerol*. 2023;158(3):180-9. DOI: 10.23736/S2784-8671.23.07639-9. PMID: 37278496.
22. Tognetti L, Cinotti E, Coriolani G, Suppa M, Perrot JL, Vascotto M, et al. Cutaneous lesions of Anderson-Fabry disease examined with a novel technique: Line-field confocal optical coherence tomography. *J Eur Acad Dermatol Venereol*. 2022;36(5):e371-e3. DOI: 10.1111/jdv.17893. PMID: 34927772.
23. Tognetti L, Carraro A, Lamberti A, Cinotti E, Suppa M, Luc Perrot J, et al. Kaposi sarcoma of the glans: New findings by line field confocal optical coherence tomography examination. *Skin Res Technol*. 2021;27(2):285-7. DOI: 10.1111/srt.12938. PMID: 32700774.
24. Martin JM, Bella-Navarro R, Jorda E. Vascular patterns in dermoscopy. *Actas Dermosifiliogr*. 2012;103(5):357-75. DOI: 10.1016/j.ad.2011.11.005. PMID: 22463770.
25. Dermoscopedia contributors. Dermoscopedia [Internet]. International Dermoscopy Society; [cited 2025 Jul 22]. Available from: https://dermoscopedia.org/
26. Reiter O, Mimouni I, Dusza S, Halpern AC, Leshem YA, Marghoob AA. Dermoscopic features of basal cell carcinoma and its subtypes: A systematic review. *J Am Acad Dermatol*. 2021;85(3):653-64. DOI: 10.1016/j.jaad.2019.11.008. PMID: 31706938.
27. Popadic M. Dermoscopic features in different morphologic types of basal cell carcinoma. *Dermatol Surg*. 2014;40(7):725-32. DOI: 10.1111/dsu.0000000000000034. PMID: 25111343.
28. Liebman TN, Jaimes-Lopez N, Balagula Y, Rabinovitz HS, Wang SQ, Dusza SW, et al. Dermoscopic features of basal cell carcinomas: differences in appearance under non-polarized and polarized light. *Dermatol Surg*. 2012;38(3):392-9. DOI: 10.1111/j.1524-4725.2011.02205.x. PMID: 22093161.
29. Minagawa A. Dermoscopy-pathology relationship in seborrheic keratosis. *J Dermatol*. 2017;44(5):518-24. DOI: 10.1111/1346-8138.13657. PMID: 28447350.
30. Zhang LW, Wang WJ, Li CH, Chen T. The string of pearls pattern in dermoscopy of a chest papule. *An Bras Dermatol*. 2020;95(3):392-3. DOI: 10.1016/j.abd.2019.06.015. PMID: 32265053.
31. Lyons G, Chamberlain AJ, Kelly JW. Dermoscopic features of clear cell acanthoma: five new cases and a review of existing published cases. *Australas J Dermatol*. 2015;56(3):206-11. DOI: 10.1111/ajd.12206. PMID: 25495637.

32. Miyake T, Minagawa A, Koga H, Fukuzawa M, Okuyama R. Histopathological correlation to the dermoscopic feature of "string of pearls" in clear cell acanthoma. *Eur J Dermatol*. 2014;24(4): 498-9. DOI: 10.1684/ejd.2014.2422. PMID: 25151914.
33. Zalaudek I, Argenziano G, Leinweber B, Citarella L, Hofmann-Wellenhof R, Malvehy J, et al. Dermoscopy of Bowen's disease. *Br J Dermatol*. 2004;150(6):1112-6. DOI: 10.1111 /j.1365-2133.2004.05924.x. PMID: 15214896.
34. Zalaudek I, Argenziano G. Glomerular vessels in Bowen's disease. *Br J Dermatol*. 2004;151(3):720. DOI: 10.1111/j.1365-2133.2004.06165.x. PMID: 15377374.
35. Argenziano G, Zalaudek I, Corona R, Sera F, Cicale L, Petrillo G, et al. Vascular structures in skin tumors: a dermoscopy study. *Arch Dermatol*. 2004;140(12):1485-9. DOI: 10.1001/archderm .140.12.1485. PMID: 15611426.
36. Greco V, Cappello M, Megna M, Costa C, Villani A, Fabbrocini G, et al. Dermoscopic patterns of intradermal naevi. *Australas J Dermatol*. 2020;61(4):337-41. DOI: 10.1111/ajd.13366. PMID: 32715462.
37. Deinlein T, Arzberger E, Zalaudek I, Massone C, Garcias-Ladaria J, Oliveira A, et al. Dermoscopic characteristics of melanoma according to the criteria "ulceration" and "mitotic rate" of the AJCC 2009 staging system for melanoma. *PLoS One*. 2017;12(4):e0174871. DOI: 10.1371/journal.pone.0174871. PMID: 28399177.
38. Sgouros D, Theofili M, Damaskou V, Theotokoglou S, Theodoropoulos K, Stratigos A, et al. Dermoscopy as a Tool in Differentiating Cutaneous Squamous Cell Carcinoma From Its Variants. *Dermatol Pract Concept*. 2021;11(2):e2021050. DOI: 10.5826/dpc.1102a50. PMID: 33954021.
39. Staibano S, Boscaino A, Salvatore G, Orabona P, Palombini L, De Rosa G. The prognostic significance of tumor angiogenesis in nonaggressive and aggressive basal cell carcinoma of the human skin. *Hum Pathol*. 1996;27(7):695-700. DOI: 10.1016/s0046-8177(96)90400-1. PMID: 8698314.
40. Vuletic MS, Jancic SA, Ilic MB, Azanjac G, Joksimovic IS, Milenkovic SM, et al. Expression of vascular endothelial growth factor and microvascular density assessment in different histotypes of basal cell carcinoma. *J BUON*. 2014;19(3):780-6. PMID: 25261667.
41. Stanton AW, Drysdale SB, Patel R, Mellor RH, Duff MJ, Levick JR, et al. Expansion of microvascular bed and increased solute flux in human Basal cell carcinoma in vivo, measured by fluorescein video angiography. *Cancer Res*. 2003;63(14): 3969-79. PMID: 12873993.
42. Chin CW, Foss AJ, Stevens A, Lowe J. Differences in the vascular patterns of basal and squamous cell skin carcinomas explain their differences in clinical behaviour. *J Pathol*. 2003;200(3): 308-13. DOI: 10.1002/path.1363. PMID: 12845626.
43. Cameron MC, Lee E, Hibler BP, Barker CA, Mori S, Cordova M, et al. Basal cell carcinoma: Epidemiology; pathophysiology; clinical and histological subtypes; and disease associations. *J Am Acad Dermatol*. 2019;80(2):303-17. DOI: 10.1016/j.jaad .2018.03.060. PMID: 29782900.
44. Pampena R, Parisi G, Benati M, Borsari S, Lai M, Paolino G, et al. Clinical and Dermoscopic Factors for the Identification of Aggressive Histologic Subtypes of Basal Cell Carcinoma. *Front Oncol*. 2020;10:630458. DOI: 10.3389/fonc.2020.630458. PMID: 33680953.
45. Gursel Urun Y, Ficicioglu S, Urun M, Can N. Clinical, Dermoscopic and Histopathological Evaluation of Basal Cell Carcinoma. *Dermatol Pract Concept*. 2023;13(1). DOI: 10.5826 /dpc.1301a4. PMID: 36892362.
46. Longo C, Lallas A, Kyrgidis A, Rabinovitz H, Moscarella E, Ciardo S, et al. Classifying distinct basal cell carcinoma subtype by means of dermoscopy and reflectance confocal microscopy. *J Am Acad Dermatol*. 2014;71(4):716-24 e1. DOI: 10.1016 /j.jaad.2014.04.067. PMID: 24928707.
47. Srivastava A, Laidler P, Davies RP, Horgan K, Hughes LE. The prognostic significance of tumor vascularity in intermediate-thickness (0.76-4.0 mm thick) skin melanoma. A quantitative histologic study. *Am J Pathol*. 1988;133(2):419-23. PMID: 3189515.
48. Schuh S, Sattler EC, Rubeck A, Schiele S, De Carvalho N, Themstrup L, et al. Dynamic Optical Coherence Tomography of Blood Vessels in Cutaneous Melanoma-Correlation with Histology, Immunohistochemistry and Dermoscopy. *Cancers (Basel)*. 2023;15(17). DOI: 10.3390/cancers15174222. PMID: 37686502.
49. Welzel J, Schuh S, De Carvalho N, Themstrup L, Ulrich M, Jemec GBE, et al. Dynamic optical coherence tomography shows characteristic alterations of blood vessels in malignant melanoma. *J Eur Acad Dermatol Venereol*. 2021;35(5):1087-93. DOI: 10.1111/jdv.17080. PMID: 33300200.
50. Dunstan S, Powe DG, Wilkinson M, Pearson J, Hewitt RE. The tumour stroma of oral squamous cell carcinomas show increased vascularity compared with adjacent host tissue. *Br J Cancer*. 1997;75(4):559-65. DOI: 10.1038/bjc.1997.98. PMID: 9052411.
51. Carmeliet P, Jain RK. Angiogenesis in cancer and other diseases. *Nature*. 2000;407(6801):249-57. DOI: 10.1038/35025220. PMID: 11001068.
52. Hutchenreuther J, Nguyen J, Quesnel K, Vincent KM, Petitjean L, Bourgeois S, et al. Cancer-associated Fibroblast-specific Expression of the Matricellular Protein CCN1 Coordinates Neovascularization and Stroma Deposition in Melanoma Metastasis. *Cancer Res Commun*. 2024;4(2):556-70. DOI: 10.1158/2767-9764.CRC-23-0571. PMID: 38363129.
53. Kavasi RM, Neagu M, Constantin C, Munteanu A, Surcel M, Tsatsakis A, et al. Matrix Effectors in the Pathogenesis of Keratinocyte-Derived Carcinomas. *Front Med (Lausanne)*. 2022;9: 879500. DOI: 10.3389/fmed.2022.879500. PMID: 35572966.
54. Mueller MM, Fusenig NE. Tumor-stroma interactions directing phenotype and progression of epithelial skin tumor cells. *Differentiation*. 2002;70(9-10):486-97. DOI: 10.1046/j.1432-0436.2002.700903.x. PMID: 12492491.
55. Lopes-Coelho F, Martins F, Pereira SA, Serpa J. Anti-Angiogenic Therapy: Current Challenges and Future Perspectives. *Int J Mol Sci*. 2021;22(7). DOI: 10.3390/ijms22073765. PMID: 33916438.